Embedded sensors for Micro Transdermal Interface Platforms (MicroTIPs)

Embedded Sensors for Micro Transdermal Interface Platforms (MicroTIPs)

Conor O'Mahony[1,*], Andrea Bocchino[1,2], Eleonora Sulas[1,2], Antonio Ciarlone[1,2], Guiseppe Giannoni[1,2], Suzanne O'Callaghan[1], Anan Kenthao[1,3], A. James P. Clover[4], Danilo Demarchi[2], Paul Galvin[1] and Konstantin Grygoryev[1]

[1]Tyndall National Institute, University College Cork, Cork, Ireland.

[2]Dipartimento di Elettronica e delle Telecomunicazioni, Politecnico di Torino, Torino, Italy.

[3]Department of Biology, Khon Kaen University, Thailand.

[4]Department of Plastic and Reconstructive Surgery, Cork University Hospital, Cork, Ireland

conor.omahony@tyndall.ie

***Abstract*—Wearable 'smart patches' of the future will incorporate microneedle technologies that painlessly interact with the body, using closed-loop theranostic systems to continuously monitor the physiological status of the body and deliver appropriate therapeutic agents when needed. Among other components, these Micro Transdermal Interface Platforms (MicroTIPs) will require embedded sensors to verify that the patch is operating as intended.**

In this paper, we integrate hollow microneedles with miniaturized pressure and impedance sensors to create an inline sensor subsystem suitable for integration with such a smart patch. Preliminary experimental work using an *ex-vivo* skin model shows that the sensors are capable of detecting microneedle skin insertion and removal, and of monitoring fluidic pressure and detecting leaks during the delivery phase.

Keywords—Microneedles, transdermal, bioMEMS, MicroTIPs

I. INTRODUCTION

In recent years there has been considerable interest in the development of microneedle technologies to overcome the skin's stratum corneum (SC) barrier in an accurate and minimally invasive manner. This outermost layer of the body is just 10-20μm thick and is largely made up of dead, keratin-filled cells (corneocytes) embedded in a lipid bilayer in a manner somewhat analogous to a bricks and mortar arrangement. The stratum corneum regulates water loss from the body and also acts as a barrier against external contaminants and environmental influences. However, it also presents a major impediment to the transdermal delivery of therapeutic agents, meaning that drug delivery via the skin is currently limited to a small number of low dose (~10 mg/day), low molecular weight (<500 Da), high lipophilicity drugs such as nicotine, scopolamine, testosterone, and fentanyl [1]. The stratum corneum layer also has a remarkably high resistance to the flow of electrical current. Many diagnostic procedures and therapies such as physiological signal monitoring or electroporation rely on external skin electrodes for the transfer of electrical signals or stimuli either to or from the body, and the high impedance of the stratum corneum greatly reduces the efficacy of such procedures [2].

Microneedle arrays are short (typically < 1000 μm in height), sharp columnar projections, made from a variety of materials and micromanufacturing processes and used for drug and vaccine delivery [3-5], physiological signal monitoring [6], and diagnostics [7, 8]. Notably, the relatively short length of microneedle arrays means that they do not stimulate nerve endings that lie deeper in the epidermis, and their use is therefore perceived as painless by the patient [9].

Microneedle technologies will eventually form the basis for wearable, intelligent, patch-like systems, capable of independently diagnosing physiological conditions and autonomously delivering relevant therapeutic doses, while simultaneously relaying patient-centric information to clinical personnel using secure wireless protocols.

These closed loop systems, which we now refer to as Micro Transdermal Interface Platforms (MicroTIPs), will have significant applications in areas such as diabetes management, stress monitoring, Parkinson's treatment and cardiac health, as well as in consumer-orientated areas such as high-performance sport and wearable wellness monitoring. MicroTIPs will be high-value and complex systems, and will lie at the opposite end of the microneedle technology spectrum to the low-cost disposable patches currently being developed for areas such as vaccine delivery [10].

MicroTIPs will require key 'building blocks' in the form of microneedle-based delivery and diagnostics modules that will be in direct contact with the body, as well as ancillary subsystems for power management, wireless

This work has been partially supported by Science Foundation Ireland under the National Access Programme and the INSIGHT Centre, by Enterprise Ireland under the Commercialisation Fund Technology Development Programme (CF/2012/2339) and the Collaborative Centre for Applied Nanotechnology, by the Higher Education Authority under the Programme for Research in Third-Level Institutions, by the EU Erasmus+ mobility scheme, and by Kon Khaen University and the Institute for the Promotion of Teaching Science and Technology of Thailand.

communications and performance validation and control. All of these must be integrated and packaged in a flexible, comfortable, and unobtrusive form factor. Significant miniaturization of communications components, battery technology and energy harvesting techniques is required to achieve this goal, as are advancements in flexible packaging formats, heterogeneous system integration, and micropump capabilities. A concept system is shown in Fig. 1.

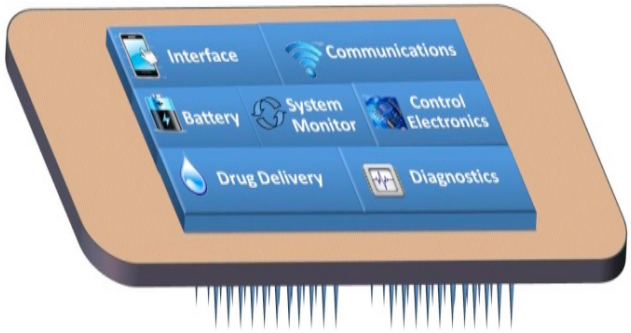

Fig. 1. Concept diagram of a future Micro Transdermal Interface Platform (MicroTIP) constructed and packaged in a wearable 'smart patch' format.

This paper concentrates on one subsystem of these platforms, which will fulfill the requirement that MicroTIPS be capable of internal validation and self-analysis of system operation and performance. It is envisaged that embedded sensors will monitor the operational parameters of the MicroTIPs patch, ensuring, for example, that the system is performing as programmed (e.g. correct delivery dosages and flowrates are achieved), that the microneedle arrays are correctly embedded in the skin and that no blockages are present, that successful therapeutic delivery and uptake has occurred, and that patient compliance targets are met.

In this work, it is shown that by using miniature pressure and impedance sensors interfaced to hollow silicon microneedle arrays, we can simultaneously monitor both the system pressure (thereby detecting leaks and/or blockages), and the quality of the skin-array contact (thereby ensuring correct application/wear and assessing patient compliance). A schematic of the prototype sensor module is shown in Fig. 2 and is intended for heterogeneous integration within a larger platform such as that illustrated in Fig. 1.

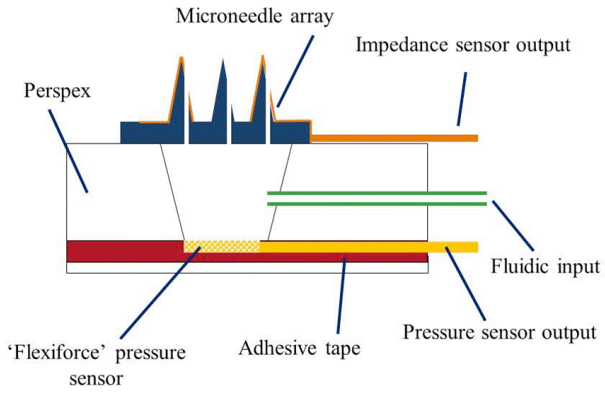

Fig. 2. Schematic of embedded sensor module for MicroTIPs.

This initial demonstrator has been validated in *ex-vivo* human skin models in a laboratory setting, and represents the first step towards an intelligent, self-regulating transdermal delivery system.

II. Experimental Details

A. Microneedle Fabrication

The microneedle arrays were fabricated using a combination of potassium hydroxide (KOH) wet etching and DRIE dry etching techniques [11-13]. Briefly, the starting material is a boron doped, 100 mm diameter monocrystalline silicon wafer, orientated in the <100> direction and onto which square oxide/nitride masks have been patterned using standard photolithography tools. These masks are aligned with the <110> crystal direction and the height of the subsequent microneedle is a linear function of the mask square side length.

The patterned silicon wafer is then etched in a 29 % w/v aqueous KOH solution until convex corner mask undercut takes place, the eight planes intersect and a needle shape is formed. This needle is comprised of eight {263} planes, a base of {212} planes and has a height:base diameter aspect ratio of 3:2. Tip sharpness is a function of mask and crystal axis alignment accuracy; tip radii are typically of the order of 50-100 nm.

Following completion of the wet-etching step, a layer of aluminium is sputtered on the front side of the wafer to act as an etch stop, and capillary tubes are then micromachined from the back side of the wafer using a dry etching tool (SPTS Technologies, Newport, UK) incorporating SF_6 and C_4F_8 etch chemistries. The resultant needle bore is 50 µm in diameter. The aluminium layer and masking layers are then stripped from both the front and back sides of the wafer, respectively. A scanning electron microscope image of a 500 µm tall hollow microneedle is shown in Fig. 3.

The octagonal microneedles are 500 µm tall, feature 71° sidewall angles, and have tip radii of the order of 50-100 nm. A microfluidic bore, 50 µm in diameter, is positioned at a lateral offset of 50 µm from the centre of the needle.

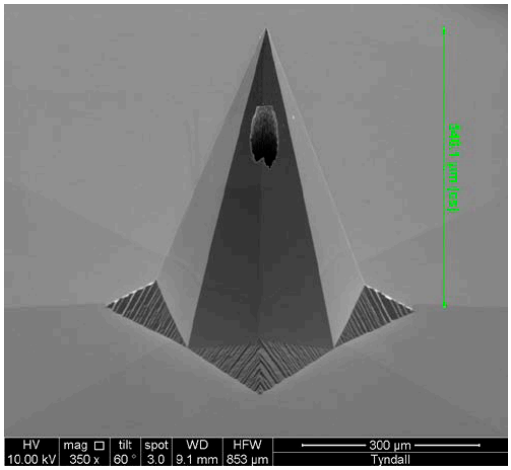

Fig. 3. SEM of a 500 µm tall, ultrasharp hollow silicon microneedle.

B. System Assembly

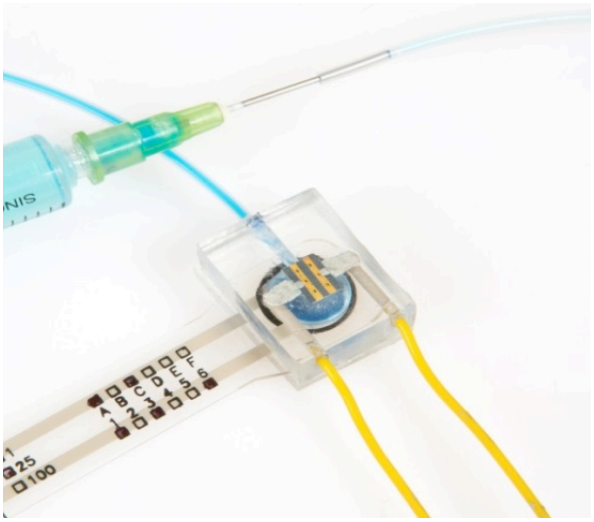

Fig. 4. A first prototype of the MicroTIPS sensor module. Electrical connections (yellow) to the impedance sensor are visible, as are the fluidic interface (blue) and the force sensor output. The microneedle array, with gold tracks for impedance monitoring, is at the centre of the system.

A prototype assembly is shown in Fig. 4, which was constructed by first dicing microneedle wafers into 3 x 2 arrays measuring 5.25 mm x 3.50 mm. Using shadow masking techniques, a 20 nm Ti/200 nm Au layer was patterned along each row to act as an impedance sensor. These arrays were bonded to a microfluidic reservoir, which was formed by first machining a cavity in a Perspex sheet; this was then bonded to a second sheet using double-sided pressure-sensitive adhesive tape. A flexible piezoresistive force sensor ('Flexiforce' A210, Tekscan Inc, Boston) was sandwiched between the two sheets to monitor the reservoir pressure. Electrical and fluidic interfaces were then added to the system, which is 7.5 mm thick and measures 21mm x 15 mm.

C. Experimental Procedure

Following protocols approved by the Clinical Research Ethics Committee of the Cork Teaching Hospitals (CREC), human skin was excised following plastic surgical operations and stored at -80 ^{o}C until needed. It was defrosted, trimmed of excess fat, cut into squares of approximately 3 cm x 3 cm, and mounted on an artificial wound closure pad to mimic the mechanical properties of underlying tissue.

Spring-loaded applicators are often used to apply microneedle devices to the skin in a consistent manner [14]. In this case, a custom-built, spring-loaded applicator, with impact energy of approximately 0.15 J/cm^2, was used to ensure repeatable and reliable skin penetration. The experimental setup is illustrated in Fig. 5.

After application, a mass of 100 *g* was placed on the needle-reservoir assembly to ensure a secure microneedle-skin interface. The resultant pressure (~ 3 kPa) is similar in magnitude to that applied by a typical ECG patch (~0.8 kPa) [15] and is required to ensure a secure microneedle-skin interface. Delivery was achieved using a syringe pump (Model KDS100, KD Scientific, MA, USA) and a solution of 1% w/v methylene blue dye was used as a model delivery solution.

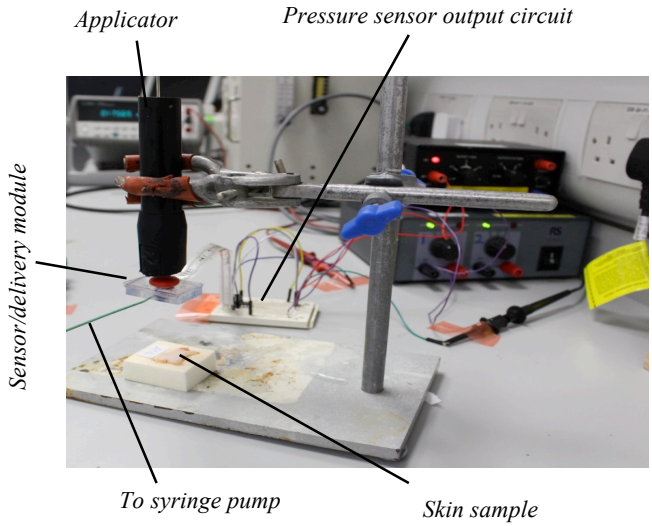

Fig. 5. Experimental setup, showing applicator, delivery module, skin sample and associated electronics.

D. Data Recording

To record pressure data, the Flexiforce force sensor was calibrated and interfaced to a signal conditioning circuit according to the manufacturer's instructions. Output voltage was measured using an Agilent 34411A digital multimeter at a frequency of 20 Hz and recorded using a PC running Agilent BenchVue software.

Impedance data was measured at 30 kHz using an Analog Devices AD5933 impedance converter system interfaced to an Arduino Uno/ATMega 328.

III. Results

A. Sensor Impedance

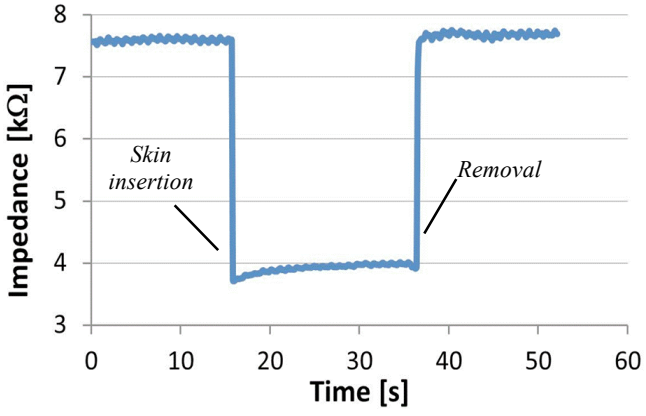

Fig. 6. Impedance profile as a function of application and removal.

Fig. 6 illustrates the impedance change before, during and after application of the sensor module to the skin using the customized applicator. A sharp drop is apparent upon skin insertion (t = 15 s), and the point of removal is similarly visible (t = 35 s).

B. System Pressure

Pressure characteristics during and after an infusion of 50 µL at a flow rate of 3 mL/hr are shown in Fig. 7. An increase of pressure with delivery volume is evident; this tended to drop slightly after delivery was complete and then decay very slowly thereafter as the fluid diffused into the tissue. The peak pressure (around 140 kPa) is similar to other reported values [16].

The 100 g mass was removed from over the sensor module at t = 400 s. A sharp drop in pressure is immediately apparent; indicating a leak of fluid from the system.

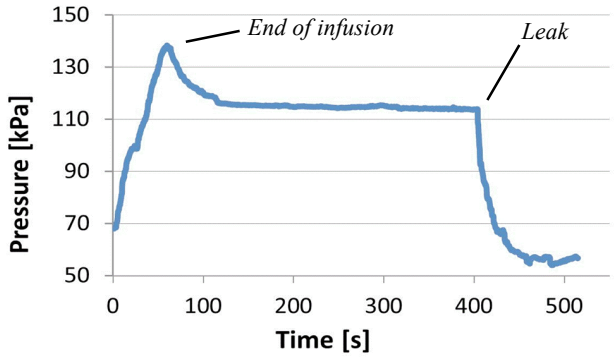

Fig. 7. Reservoir pressure as a function of infusion time. Note the sharp pressure drop at t = 400 s, indicating the presence of a leak at the microneedle-skin interface. Total delivery volume is 50µL at a flowrate of 3 mL/hour.

C. Skin Penetration and Delivery Validation

Fig. 8 illustrates the site of insertion of a row of microneedles. The transient pores created by the needles are clearly visible, as is the methylene blue dye solution beneath the skin's surface, confirming fluidic delivery to the region beneath the stratum corneum.

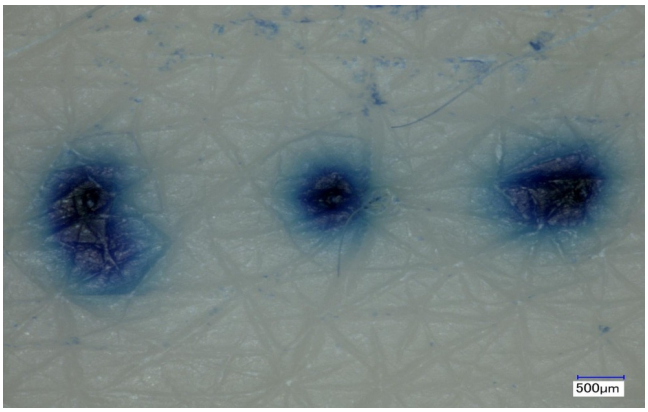

Fig. 8. *En face* image of microneedle delivery site.

IV. Discussion

It is clear from our experimental work that a mechanically secure needle-skin interface is key to successful drug delivery. The high pressures evident during the delivery phase mean that fluid will easily leak without appropriate external forces being applied to the site to keep the microneedle array in place, and this will be a major consideration during development of the skin adhesive tapes that will be used to robustly adhere the device to the body. Our integrated impedance sensor will assist with monitoring of this interface quality, and future work will develop continuous skin insertion depth sensors instead of the initial binary in/out sensor presented here.

Performance and integration may also be improved by further miniaturization and thinning of the module, which will reduce fluidic dead volume and facilitate easier integration with the platform. This is achievable in the first instance by employing smaller pressure sensors and a thinner fluidic housing fabricated using additive manufacturing tools..

Future work will also continue to assess the microfluidic delivery performance envelope, to develop miniaturized electronics and micropumps, and to characterize the reliability of the system in an *in-vivo*, ambulatory setting.

V. Conclusion

For the first time, a microneedle-based transdermal delivery system featuring embedded performance monitoring sensors has been demonstrated. Using an ultrathin pressure sensor and a customized impedance sensor, we have shown that it is possible to simultaneously measure both the fluidic pressure of the delivery system and the quality of the microneedle-skin contact during the delivery phase. Typical delivery volumes are of the order of 50-150 µL at flowrates of a few mL/hour, resulting in peak pressures of approximately 140 kPa.

The work represents an important step on the roadmap towards the realization of high-value Micro Transdermal Interface Platforms (MicroTIPs).

References

[1] T. Tanner and R. Marks, "Delivering drugs by the transdermal route: review and comment," Skin. Res. Technol., vol. 14, pp. 249-60, 2008.

[2] J. Webster, Medical instrumentation: application and design. Hoboken, NJ: John Wiley & Sons, 2009.

[3] Y.-C. Kim, J.-H. Park, and M. R. Prausnitz, "Microneedles for drug and vaccine delivery," Adv. Drug Deliv. Rev., vol. 64, pp. 1547-1568, 2012.

[4] R. J. Pettis and A. J. Harvey, "Microneedle delivery: clinical studies and emerging medical applications," Ther. Deliv., vol. 3, pp. 357-371, 2012.

[5] K. van der Maaden, W. Jiskoot, and J. Bouwstra, "Microneedle technologies for (trans) dermal drug and vaccine delivery," J. Control. Rel., vol. 161, pp. 645-655, 2012.

[6] C. O'Mahony, F. Pini, A. Blake, C. Webster, J. O'Brien, and K. G. McCarthy, "Microneedle-based electrodes with integrated through-silicon via for biopotential recording," Sens. Actuators A Phys., vol. 186, pp. 130-136, 2012.

[7] C. Barrett, K. Dawson, C. O'Mahony, and A. O'Riordan, "Development of low cost rapid fabrication of sharp polymer microneedles for in vivo glucose biosensing applications," ECS J. Solid State Sci. Technol., vol. 4, pp. S3053-S3058, 2015.

[8] R. F. Donnelly, K. Mooney, E. Caffarel-Salvador, B. M. Torrisi, E. Eltayib, and J. C. McElnay, "Microneedle-mediated minimally invasive patient monitoring," Ther. Drug Monit., vol. 36, pp. 10-7, 2014.

[9] M. Haq, E. Smith, D. John, M. Kalavala, C. Edwards, A. Anstey, *et al.*, "Clinical administration of microneedles: skin puncture, pain and sensation," Biomed. Microdevices, vol. 11, pp. 35-47, 2009.

[10] E. Jacoby, C. Jarrahian, H. F. Hull, and D. Zehrung, "Opportunities and challenges in delivering influenza vaccine by microneedle patch," Vaccine, vol. 33, pp. 4699-4704, 2015.

[11] J. O'Brien, M. Bedoni, A. Blake, J. Scully, E. Forvi, M. Casella, *et al.*, "Hollow Microneedles for Pain-Free Drug Delivery," presented at the 20th Micromechanics and Microsystems Workshop Europe, Toulouse, France, 20th-22nd September, 2009.

[12] N. Wilke and A. Morrissey, "Silicon microneedle formation using modified mask designs based on convex corner undercut," J. Micromech. Microeng., vol. 17, p. 238, 2007.

[13] N. Wilke, M. L. Reed, and A. Morrissey, "The evolution from convex corner undercut towards microneedle formation: theory and experimental verification," J. Micromech. Microeng., vol. 16, p. 808, 2006.

[14] T. R. Singh, N. J. Dunne, E. Cunningham, and R. F. Donnelly, "Review of patents on microneedle applicators," Recent Pat. Drug Deliv. Formul., vol. 5, pp. 11-23, 2011.

[15] C. O'Mahony, K. Grygoryev, A. Ciarlone, G. Giannoni, A. Kenthao, and P. Galvin, "Design, fabrication and skin-electrode contact analysis of polymer microneedle-based ECG electrodes," J. Micromech. Microeng., vol. in press, 2016.

[16] W. Martanto, J. S. Moore, O. Kashlan, R. Kamath, P. M. Wang, J. M. O'Neal, *et al.*, "Microinfusion using hollow microneedles," Pharm. Res., vol. 23, pp. 104-13, 2006.